51 Rossel M, Capecchi MR. Mice mutant for both Hoxa1 and Hoxb1 show extensive remodeling of the hindbrain and defects in craniofacial development. *Development* 1999; **126**: 5027–40
52 Tischfield MA, Bosley TM, Salih MAM, Alorainy IA, Sener EC, Nester MJ, Oystreck DT, Chan WM, Andrews C, Erickson RP, Engle EC. Homozygous HOXA1 mutations disrupt human brainstem, inner ear, cardiovascular and cognitive development. *Nat Genet* 2005; **37**: 1035–7
53 Kauselmann G, Weiler M, Wuff P, Jessberger S, Konietzko U, Scafidi J, Staubli U, Bereiter-Hahn J, Strebhardt K, Kuhl D. The polo-like protein kinases Fnk and Snk associate with a Ca^{2+}- and integrin-binding protein and are regulated dynamically with synaptic plasticity. *EMBO J* 1999; **18**: 5528–39
54 Kim NK, Ahn JY, Song J, Kim JK, Han JH, An HJ, Chung HM, Joo JY, Choi JU, Lee KS, Roy R, Oh D. Expression of the DNA repair enzyme, N-methylpurine-DNA glycosylase (MPG) in astrocytic tumors. *Anticancer Res* 2003; **23**: 1417–23
55 Zahn R, Liu A, Lührs T, von Schroetter C, Garcia FL, Billeter M, Calzolai L, Wider G, Wüthrich K. NMR solution structure of the human prion protein. *Proc Natl Acad Sci USA* 2000; **97**: 145–50
56 Crozet C, Vézilier J, Delfieu V, Nishimura T, Onodera T, Casanova D, Lehmann S, Béranger F. The truncated 23–230 form of the prion protein localizes to the nuclei of inducible cell lines independently of its nuclear localization signals and is not cytotoxic. *Mol Cell Neurosci* 2006; **32**: 315–23
57 Gu Y, Hinnerwisch J, Fredricks R, Kalepu S, Mishra RS, Singh N. Identification of cryptic nuclear localization signals in the prion protein. *Neurobiol Dis* 2003; **12**: 133–49
58 Mangé A, Crozet C, Lehmann S, Béranger F. Scrapie-like prion protein is translocated to the nuclei of infected cells independently of proteasome inhibition and interacts with chromatin. *J Cell Sci* 2004; **117**: 2411–16
59 Kovacs GG, Voigtländer T, Hainfellner JA, Budka H. Distribution of intraneuronal immunoreactivity for the prion protein in human prion diseases. *Acta Neuropathol* 2002; **104**: 320–6
60 Gabus C, Auxilien S, Péchoux C, Dormont D, Swietnicki W, Morillas M, Surewicz W, Nandi P, Darlix JL. The prion protein has DNA strand transfer properties similar to retroviral nucleocapsid protein. *J Mol Biol* 2001; **307**: 1011–21
61 Ma J, Wollmann R, Lindquist S. Neurotoxicity and neurodegeneration when PrP accumulates in the cytosol. *Science* 2002; **298**: 1781–5
62 Ma J, Lindquist S. Conversion of PrP to a self-pertuating PrP^{Sc}-like conformation in the cytosol. *Science* 2002; **298**: 1785–8
63 Yuan J, Xiao X, McGeehan J, Dong Z, Cali I, Fujioka H, Kong Q, Kneale G, Gambetti P, Zou WQ. Insoluble aggregates and protease-resistant conformers of prion protein in uninfected human brains. *J Biol Chem* 2006; **46**: 34848–58
64 Chen S, Mangé A, Dong L, Lehmann S, Schachner M. Prion protein as trans-interacting partner for neurons is involved in neurite outgrowth and neuronal survival. *Mol Cell Neurosci* 2003; **22**: 227–33
65 Spudich A, Frigg R, Kilic E, Kilic U, Oesch B, Raeber A, Bassetti CL, Hermann DM. Aggravation of ischemic brain injury by prion protein deficiency: role ERK-1/-2 and STAT-1. *Neurobiol Dis* 2005; **20**: 442–9
66 Weise J, Sandau R, Schwarting S, Crome O, Wrede A, Schulz-Schaeffer W, Zerr I, Bahr M. Deletion of cellular prion protein results in reduced Akt activation, enhanced postischemic caspase-3 activation, and exacerbation of ischemic brain injury. *Stroke* 2006; **37**: 1296–300
67 Carimalo J, Cronier S, Petit G, Peyrin JM, Boukhtouche F, Arbez N, Lemaigre-Dubreuil Y, Brugg B, Miquel MC. Activation of the JNK-c-Jun pathway during the early phase of neuronal apoptosis induced by PrP106-126 and prion infection. *Eur J Neurosci* 2005; **21**: 2311–19
68 Satoh J, Kuroda Y, Katamine S. Gene expression profile in prion protein-deficient fibroblasts in culture. *Am J Pathol* 2000; **157**: 59–68

Received 26 January 2008
Accepted after revision 7 February 2008

Supplementary material

The following supplementary material is available for this article online:

Table S1. Primers utilized for PCR in the present study.
Table S2. The complete list of the proteins immobilized on a human protein microarray utilized in the present study.

The supplementary material is available as part of the online article from: http://www.blackwell-synergy.com/doi/abs/10.1111/j.1365-2990.2008.00947.x

Please note: Blackwell Publishing is not responsible for the content or functionality of any supplementary materials supplied by the authors. Any queries (other than missing material) should be directed to the corresponding author for the article.

Multiple Sclerosis

http://msj.sagepub.com

Molecular network of the comprehensive multiple sclerosis brain-lesion proteome

JI Satoh, H Tabunoki and T Yamamura

Mult Scler 2009; 15; 531
DOI: 10.1177/1352458508101943

The online version of this article can be found at:
http://msj.sagepub.com/cgi/content/abstract/15/5/531

Published by:
SAGE
http://www.sagepublications.com

RESEARCH PAPER *Multiple Sclerosis* 2009; **15:** 531–541

Molecular network of the comprehensive multiple sclerosis brain-lesion proteome

JI Satoh[1,2], H Tabunoki[1] and T Yamamura[2]

Background A recent proteomics study of multiple sclerosis (MS) lesion-specific proteome profiling clearly revealed a pivotal role of coagulation cascade proteins in chronic active demyelination. However, among thousands of proteins examined, nearly all of remaining proteins are yet to be characterized in terms of their implications in MS brain-lesion development.

Methods By the systems biology approach using four different pathway analysis tools of bioinformatics, we studied molecular networks and pathways of the proteome dataset of acute plaques, chronic active plaques (CAP), and chronic plaques (CP).

Results The database search on Kyoto Encyclopedia of Genes and Genomes (KEGG) and protein analysis through evolutionary relationships (PANTHER) indicated the relevance of extracellular matrix (ECM)–mediated focal adhesion and integrin signaling to CAP and CP proteome. KeyMolnet disclosed a central role of the complex interaction among diverse cytokine signaling pathways in brain-lesion development at all disease stages, as well as a role of integrin signaling in CAP and CP. Ingenuity pathway analysis (IPA) identified the network constructed with a wide range of ECM components, such as collagen, type I α1, type I α2, type VI α2, type VI α3, fibronectin 1, fibulin 2, laminin α1, vitronectin, and heparan sulfate proteoglycan, as one of the networks highly relevant to CAP proteome.

Conclusions Although four distinct platforms produced diverse results, they commonly suggested a role of ECM and integrin signaling in development of chronic lesions of MS. These *in silico* observations indicate that the selective blockade of the interaction between ECM and integrins in brain lesions *in situ* would be a target for therapeutic intervention in MS. *Multiple Sclerosis* 2009; **15:** 531–541. http://msj.sagepub.com

Key words: extracellular matrix; multiple sclerosis; pathway analysis; proteome; systems biology

Introduction

Multiple sclerosis (MS) is an inflammatory demyelinating disease of the central nervous system (CNS) presenting with relapsing-remitting and progressive clinical courses. An autoimmune process triggered by a complex interplay between genetic and environmental factors may mediate MS, although the causative agents have not yet been identified. Pathologically, MS shows remarkable heterogeneity in inflammatory demyelination, astrogliosis, and axonal degeneration [1]. Even though various drugs are lined up in clinical trials, currently, treatment options with limited efficacies, including interferon-β, glatiramer acetate, and mitoxantrone are available for ordinary clinical practice of MS [2].

The completion of the Human Genome Project in 2003 allows us to systematically characterize the comprehensive disease-associated profiles of the whole human genome [3]. The global analysis of transcriptome, proteome, protein interactome, and metabolome helps us identify disease-specific molecular signatures and biomarkers for diagnosis and prediction of prognosis, and would broaden the spectrum of molecular mechanism-based therapy for MS [4,5]. Actually, the comprehensive gene expression profiling of MS brain tissues and peripheral blood lymphocytes by DNA microarray identified a battery of genes aberrantly regulated in MS, whose role has not been previously predicted during its pathogenesis [6,7]. A recent proteomics study of MS lesion-specific proteome profiling showed

[1]Department of Bioinformatics and Molecular Neuropathology, Meiji Pharmaceutical University, Tokyo, Japan
[2]Department of Immunology, National Institute of Neuroscience, NCNP, Tokyo, Japan
Correspondence to: Jun-Ichi Satoh, Department of Bioinformatics and Molecular Neuropathology, Meiji Pharmaceutical University, Tokyo, Japan. Email: satoj@my-pharm.ac.jp
Received 23 July 2008; accepted 12 November 2008

10.1177/1352458508101943

that overproduction of tissue factor and protein C inhibitor plays a central role in molecular events ongoing in chronic active plaques (CAP) [8]. *In vivo* administration of coagulation cascade inhibitors really reduced the clinical severity in a mouse model of experimental autoimmune encephalomyelitis (EAE), supporting the view that the blockade of the coagulation cascade would be a potential approach for the treatment of MS [8]. However, among thousands of proteins this study examined, nearly all of remaining proteins were left behind to be characterized in terms of their implications in MS brain-lesion development.

Since the global expression analysis of transcriptome and proteome usually produces high-throughput experimental data at a time, it is often difficult to find out the meaningful biological implications of the dataset. Recent advances in systems biology enable us to illustrate the cell-wide map of the complex molecular interactions by using the literature-based knowledgebase of molecular pathways [9,10]. In the scale-free molecular network, targeted disruption of limited numbers of critical components, on which the biologically important molecular connections concentrate, could disturb the whole cellular function by destabilizing the network [11]. From this point of view, the integration of comprehensive transcriptome and proteome data of disease-affected tissues with underlying molecular networks could provide the rational approach not only to characterize disease-relevant pathways but also to achieve the network-based choice of effective drug targets. By using four different pathway analysis tools of bioinformatics, this study was designed to characterize molecular networks and pathways of MS lesion-specific proteome data of Han, *et al.* [8]. Although the analysis by distinct platforms did not lead to fully identical results, they commonly suggested a role of extracellular matrix (ECM) and integrin signaling in chronic lesions of MS. These *in silico* observations indicate that ECM and integrins would be a target candidate for designing therapeutic intervention in MS.

Databases and methods

The dataset of the comprehensive MS brain-lesion proteome

In the original dataset of Han, *et al.* [8], fresh-frozen brain autopsy samples were collected from six MS patients of different clinical subtypes, acute, chronic, progressive, secondary progressive, or chronic progressive, with ages 27–54, and from two age-matched control subjects free of neurological diseases. The postmortem interval of each case ranged from 4 to 24 h. Multiple sclerosis lesions were classified into three distinct categories: acute plaques (AP), CAP (chronic active plaques), or chronic plaques (CP), based on histological evaluation of the disease activity, briefly as follows: AP showed characteristics of acute ongoing inflammation, edema, and active demyelination. CAP was characterized by chronic demyelination with active inflammation at the lesion edges, whereas CP represented chronic inactive demyelination accompanied by profound astrogliosis. Protein samples were prepared from small pieces of brain tissues isolated by laser-captured microdissection, and the tissue pieces were characterized separately by the standard histological examination. The proteins were separated on one-dimensional SDS-PAGE (sodium dodecyl sulfate-polyacrylamide gel electrophoresis) gels. Then, the protein bands were dissected and digested in a gel with trypsin, and peptide fragments were processed for mass spectrometric analysis several times to obtain a saturation point. Among 2,574 proteins determined with high confidence, the application of a computational data exploration program named INTERSECT/INTERACT identified 158, 416, and 236 lesion-specific proteins that were detected exclusively in AP, CAP, and CP, respectively. In this study, we tentatively called them as the comprehensive MS brain-lesion proteome dataset.

Conversion of protein IDs into Entrez Gene IDs and KEGG IDs

We converted the protein IDs listed in the dataset described above into the corresponding the National Center for Biotechnology Information (NCBI) Entrez Gene IDs, Gene Symbols, and Kyoto Encyclopedia of Genes and Genomes (KEGG) IDs by searching them on the UniProt knowledgebase (http://www.expasy.org/sprot).

Molecular network analysis

To identify biologically relevant molecular pathways from large-scale proteome data, we have undertaken the systems biology approach. We analyzed them by using four distinct pathway analysis tools endowed with a comprehensive knowledgebase which are as follows: KEGG (http://www.kegg.jp), the protein analysis through evolutionary relationships (PANTHER) classification system (http://www.pantherdb.org), Ingenuity pathways analysis (IPA) (Ingenuity Systems, Redwood City, CA; http://www.ingenuity.com), and KeyMolnet (Institute of Medicinal Molecular Design, Tokyo, Japan; http://www.immd.co.jp).

By importing the list of KEGG IDs, we studied molecular pathways on KEGG, a public database that systematically integrates genomic and chemical information to create the whole biological system *in silico*. KEGG contains manually curated reference pathways that cover a wide range of metabolic, genetic, environmental, and cellular processes, and human diseases [12]. Currently, KEGG contains 90,931 pathways generated from 371 reference pathways. PANTHER, a public database generated by computational algorithms that relate the evolution of protein sequence to the evolution of protein functions and biological roles, provides a structured representation of protein function in the context of biological reaction networks [13]. Currently, PANTHER includes the information on 165 regulatory and metabolic pathways, manually curated by expert biologists. PANTHER visualizes pathway maps with the format compatible with the Systems Biology Markup Language (SBML) standard. By uploading the list of Entrez Gene IDs, PANTHER identifies the genes in terms of over- or under-representation in canonical pathways, followed by statistical evaluation by multiple comparison with a Bonferroni correction.

IPA is a commercial tool built upon a knowledgebase that contains approximately 1,600,000 biological and chemical interactions and functional annotations with scientific evidence. They are collected from more than 300 selected articles, textbooks, and other data sources, manually curated by expert biologists. By uploading the list of Entrez Gene IDs, the network-generation algorithm identifies focused genes integrated in a global molecular network [14]. IPA calculates the score *P*-value, the statistical significance of association between the genes and the network by the Fisher's exact test.

KeyMolnet is a commercial database, composed of knowledge-based contents on relationships among human genes, molecules, diseases, pathways, and drugs, curated by expert biologists. They are categorized into the core contents that are collected from selected review articles with the highest reliability or the secondary contents extracted from abstracts of PubMed database and Human Reference Protein database. By importing the list of Entrez gene ID, KeyMolnet automatically provides corresponding molecules as a node on networks [15]. The "N-points to N-points" network-search algorithm identifies the molecular network constructed by the shortest route connecting the start point molecules and the end point molecules. The generated network was compared side by side with 346 human canonical pathways of the KeyMolnet library. The algorithm counting the number of overlapping molecular relations between the extracted network and the canonical pathway makes it possible to identify the canonical pathway showing the most significant contribution to the extracted network. The significance in the similarity between both is scored following the formula, where O = the number of overlapping molecular relations between the extracted network and the canonical pathway, V = the number of molecular relations located in the extracted network, C = the number of molecular relations located in the canonical pathway, T = the number of total molecular relations composed of approximately 90,000 sets, and the X = the sigma variable that defines coincidence.

$$\text{Score} = -\log_2(\text{Score}(p))$$
$$\text{Score}(p) = \sum_{x=0}^{\text{Min}(C,V)} f(x)$$
$$f(x) = {}_C C_x \cdot {}_{T-C} C_{V-x} / {}_T C_V$$

Results

KEGG and PANTHER searches elucidated a role of ECM-mediated cell adhesion in chronic lesions of MS

First of all, we converted all protein IDs listed in the original database [8] into the corresponding NCBI Entrez Gene IDs, Gene Symbols, and KEGG IDs by searching them on the UniProt knowledgebase. After the removal of unaccepted and redundant IDs, we finally identified 155, 407, and 232 Entrez Gene IDs and KEGG IDs from the AP, CAP, and CP-specific proteome data, respectively. They are listed in Supplementary Tables 1–3*.

When the KEGG IDs of the proteome were uploaded onto the 'Search Objects in Pathway' tool of the KEGG database, the vast majority of AP, CAP, or CP-specific proteins was not mapped on any KEGG human reference pathways (Table 1). However, a battery of CAP-specific proteins were categorized as those located in the pathways linked to focal adhesion (KEGG pathway ID: hsa04510), cell communication (hsa01430), ECM-receptor interaction (hsa04512), purine metabolism (hsa00230), and other biological pathways (not shown). Likewise, a panel of CP-specific proteins was found to be involved in the pathways linked to focal adhesion, regulation of actin cytoskeleton (hsa04810), oxidative phosphorylation (hsa00190), and cell communication (Table 1). These results are derived chiefly from enhanced production and deposition of ECM and receptor components, including collagen, fibronectin, vitronection, integrin, and laminin in CAP and CP lesions. In contrast, relatively small numbers of AP-specific proteins were mapped on the

*Supplementary Tables 1–4 are available online at http://msj.sagepub.com/

Table 1 The molecular pathway relevant to multiple sclerosis (MS) brain-lesion proteome suggested by KEGG search

Stage	Rank	Functional category (KEGG Pathway ID)	Genes classified
AP	1	Unclassified	123 genes
	2	Oxidative phosphorylation (hsa00190)	NDUFS7, NDUFB9, ATP4A, ATP6V0C
	3	Regulation of actin cytoskeleton (hsa04810)	FGD1, ITGB4, SSH1, ACTA1
CAP	1	Unclassified	281 genes
	2	Focal adhesion (hsa04510)	COL1A1, COL1A2, COL5A2, COL6A2, COL6A3, FN1, LAMA1, MYLK, SHC3, PPP1CA, PARVA, PRKCB1, MYL7, RAC3, SPP1, SRC, THBS1, VTN
	3	Cell communication (hsa01430)	NES, COL1A, COL1A2, COL5A2, COL6A2, COL6A3, KRT78, FN1, GJA1, LAMA1, KRT3, SPP1, THBS1, VTN
	4	ECM-receptor interaction (hsa04512)	COL1A1, COL1A2, COL5A2, COL6A2, COL6A3, FN1, LAMA1, HSPG2, SPP1, THBS1, VTN
	5	Purine metabolism (hsa00230)	ADCY5, TYMP, NT5E, PDE2A, PDE3B, PDE4A, PDE4B, PRPS2, GMPS, ENTPD1
CP	1	Unclassified	166 genes
	2	Focal adhesion (hsa04510)	COL4A2, COL6A1, CRK, FYN, ITGA6, LAMB2, LAMC1, PIK3CA, ZYX
	3	Regulation of actin cytoskeleton (hsa04810)	WASF2, BAIAP2, CRK, ITGA6, PIK3CA, TIAM1, MYH14, ARHGEF7
	4	Oxidative phosphorylation (hsa00190)	NDUFB6, NDUFB8, NDUFS5, ATP5I, ATP6V1F
	5	Cell communication (hsa01430)	COL4A2, COL6A1, ITGA6, LAMB2, LAMC1

The list of KEGG IDs of MS brain-lesion proteome was uploaded onto the 'Search Objects in Pathway' tool of the KEGG database. Top 2 for AP and top 4 for CAP and CP of human reference pathways relevant to the proteome data are shown with KEGG pathway IDs and the list of genes classified.
Abbreviations: AP, acute plaques; CAP, chronic active plaques; and CP, chronic plaques.

pathways, such as oxidative phosphorylation and regulation of actin cytoskeleton (Table 1). Thus, the KEGG search suggested that the biological process of ECM and integrin-mediated cell adhesion and communication plays a role in chronic lesions of MS.

When the Entrez Gene IDs of the proteome were imported into the 'Gene Expression Data Analysis' tool of the PANTHER database, the vast majority of AP, CAP, or CP-specific proteins were not mapped on any PANTHER canonical pathways in comparison with a reference set of NCBI human genes (Table 2). However, PANTHER identified a statistically significant relationship between a set of CAP proteins and signaling pathways of chemokines and cytokines, integrin (Figure 1), muscarinic and nicotinic acetylcholine receptors (Table 2). PANTHER suggested an involvement of integrin signaling in CP, but identified no pathways relevant to AP (Table 2). Thus, the PANTHER search indicated that integrin signaling plays a role in both CAP and CP, whereas inflammation mediated by chemokine and cytokine signaling plays a predominant role in CAP.

Table 2 The molecular pathway relevant to MS brain-lesion proteome suggested by PANTHER search

Stage	Rank	Functional category	Number of genes classified	Human reference genes	*P*-value
AP	1	Unclassified	120	22436	6.89E-02 (NS)
CAP	1	Unclassified	321	22436	1,73E-04
	2	Inflammation mediated by chemokine and cytokine signaling pathway	17	315	2,63E-03
	3	Integrin signaling pathway	14	227	3,55E-03
	4	Muscarinic acetylcholine receptor 1 and 3 signaling pathway	7	62	1,17E-02
	5	Nicotinic acetylcholine receptor signaling pathway	8	91	2,03E-02
CP	1	Unclassified	182	22436	9,75E-03
	2	Integrin signaling pathway	9	227	4,33E-02

The list of Entrez Gene IDs of MS brain-lesion proteome was uploaded onto the 'Gene Expression Data Analysis' tool of the PANTHER classification system by comparing with a reference set of NCBI human genes. The canonical pathways relevant to the proteome data are shown with the number of genes classified and *P*-value evaluated by multiple comparison with a Bonferroni correction.
Abbreviations: AP, acute plaques; CAP, chronic active plaques; CP, chronic plaques; and NS, not significant.

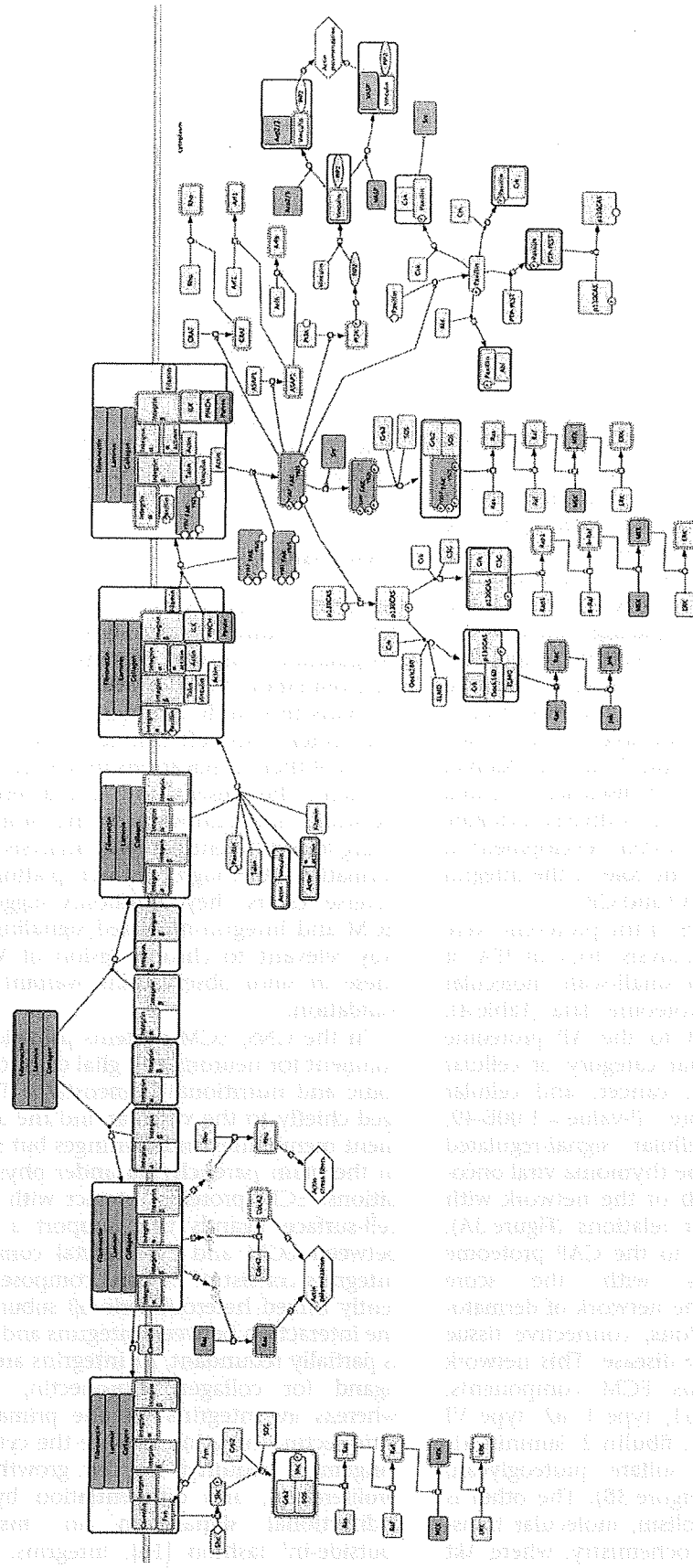

Figure 1 Integrin signaling pathway relevant to CAP proteome suggested by PANTHER. The list of Entrez Gene IDs of CAP-specific proteome was uploaded onto the 'Gene Expression Data Analysis' tool of the PANTHER classification system by comparing them with a reference set of NCBI human genes. Integrin signaling pathway was identified as one of canonical pathways statistically relevant to the CAP proteome (Table 2). The pathway is illustrated as the map compatible with the Systems Biology Markup Language (SBML) standard. The molecules colored in pink represent those included in the gene list (Supplementary Table 2). They are composed of fibronectin (Gene symbol: FN1), laminin (LAMA1), collagen (COL1A1, COL1A2, COL5A2, COL6A2, COL6A3), Rac (RAC3), MEK (MAP2K4), FAK (PTK2B), parvin (PARVA), Src (SRC), Jnk (MAP2K4), Arp2/3 (ARPC1A), and VASP (ENAH).

KeyMolnet and IPA searches disclosed a role of the complex interaction of diverse intracellular signaling pathways in brain lesion development of MS

Next, we investigated molecular networks of MS brain proteome by utilizing two different commercial platforms. When the Entrez Gene IDs of the proteome were uploaded onto the "N-points to N-points" search tool of KeyMolnet, it extracted highly complex large-scale molecular networks of the AP, CAP, and CAP-specific proteome (Figure 2). The network of the AP, CAP, or CP proteome is composed of 777, 1,120, or 952 fundamental nodes with 1,892, 2,772, or 2,279 molecular relations, respectively. The statistical evaluation indicated that the top five most relevant molecular networks include IL-4, IL-6, IL-2, and catenin signaling pathways and transcriptional regulation by STAT (signal transducer and activator of transcription) for the AP proteome, PI3K, IL-4, type I IFN, and IL-6 signaling pathways and transcriptional regulation by STAT for the CAP proteome, and IL-4, hepatocyte growth factor (HGF), TCR (T cell receptor), integrin and IL-6 signaling pathways for the CP proteome (Table 3). It is worthy to note that the integrin signaling pathway was ranked as the sixth relevant pathway to the CAP proteome with *P*-value of the score = 2.13E-012. Considerable overlap existed in the results of PANTHER (Table 2) and KeyMolnet (Table 3). The KeyMolnet search disclosed a central role of the complex interaction of diverse cytokine signaling pathways in brain lesion development at all disease stages of MS, and the role of the integrin signaling pathway in both CAP and CP.

When the Entrez Gene IDs of the proteome were imported into the 'Core Analysis' tool of IPA, it highlighted several units of small-scale molecular networks relevant to the proteome data (Table 4). The network most relevant to the AP proteome was linked to the functional category of cellular assembly and organization, cancer, and cellular movement with the score *P*-value = 1.00E-49, where both ERK (extracellular signal-regulated kinase) and Akt (V-akt murine thymoma viral oncogene homolog) act as a hub of the network with highly connected molecular relations (Figure 3A). The network most relevant to the CAP proteome included two categories with the score *P*-value = 1.00E-47. One is the network of dermatological diseases and conditions, connective tissue disorders, and inflammatory disease. This network is constructed with various ECM components, including collagen, type I α1, type I, α2, type VI α2, type VI α3, fibronectin 1, fibulin 2, laminin α1, vitronectin, and heparan sulfate proteoglycan, where ERK acts as a hub (Figure 3B). The other is the network of lipid metabolism, molecular transport, and small molecule biochemistry, where Akt acts as a hub (Figure 3C). The network most relevant to the CP proteome was linked to cell cycle, cell morphology, and cell-to-cell signaling and interaction with the score *P*-value = 1.00E-50, where NF-κB (nuclear factor-kappa B) serves as a hub (Figure 3D). Overall, the biological processes involved in cellular assembly, organization, growth, proliferation, movement, and development are key functional categories shared by AP and CP molecular networks (Table 4). IPA also identified in the canonical pathways relevant to the proteome data. Both calcium signaling and oxidative phosphorylation were categorized as those relevant to AP and CAP proteome, whereas the actin cytoskeleton signaling pathway was considered as the important pathway in both CAP and CP (Table 5). Considerable overlap existed in the results of KEGG (Table 1) and IPA (Table 5).

Discussion

A recent proteomics study of MS lesion-specific proteome profiling clearly showed a pivotal role of coagulation cascade proteins in chronic active demyelination [8]. However, among thousands of proteins this study examined, nearly all of remaining proteins are left behind to be characterized in terms of their implications in MS brain-lesion development. The present study characterized molecular networks and pathways of the proteome data by using four different pathway analysis tools of bioinformatics. Although distinct platforms produced diverse results, they commonly suggested a role of ECM and integrin-mediated signaling as the pathway relevant to chronic lesion of MS. Therefore, these *in silico* observations warrant experimental validation.

In the CNS, ECM proteins provide a microenvironment for neurons and glial cells to maintain the ionic and nutritional homeostasis. They are localized chiefly to the vascular and the astroglial basement membranes and meninges but scarcely found in the brain parenchyma under physiological conditions. ECM proteins interact with integrins, the cell-surface ligands that support a physical link between ECM and cytoskeletal components [16]. Integrins consist of 24 pairs composed of noncovalently linked heterodimeric αβ subunits. Although the interaction between integrins and ECM proteins is partially redundant, β1 integrins are the principal ligand for collagen, fibronectin, and laminin, whereas αv integrins are the primary ligand for vitronectin. Integrins regulate the cytoskeletal rearrangement required for cell growth, movement, proliferation, and differentiation by transducing bidirectional signals in an 'inside-out' and 'outside-in' fashion [16]. Integrins, expressed on

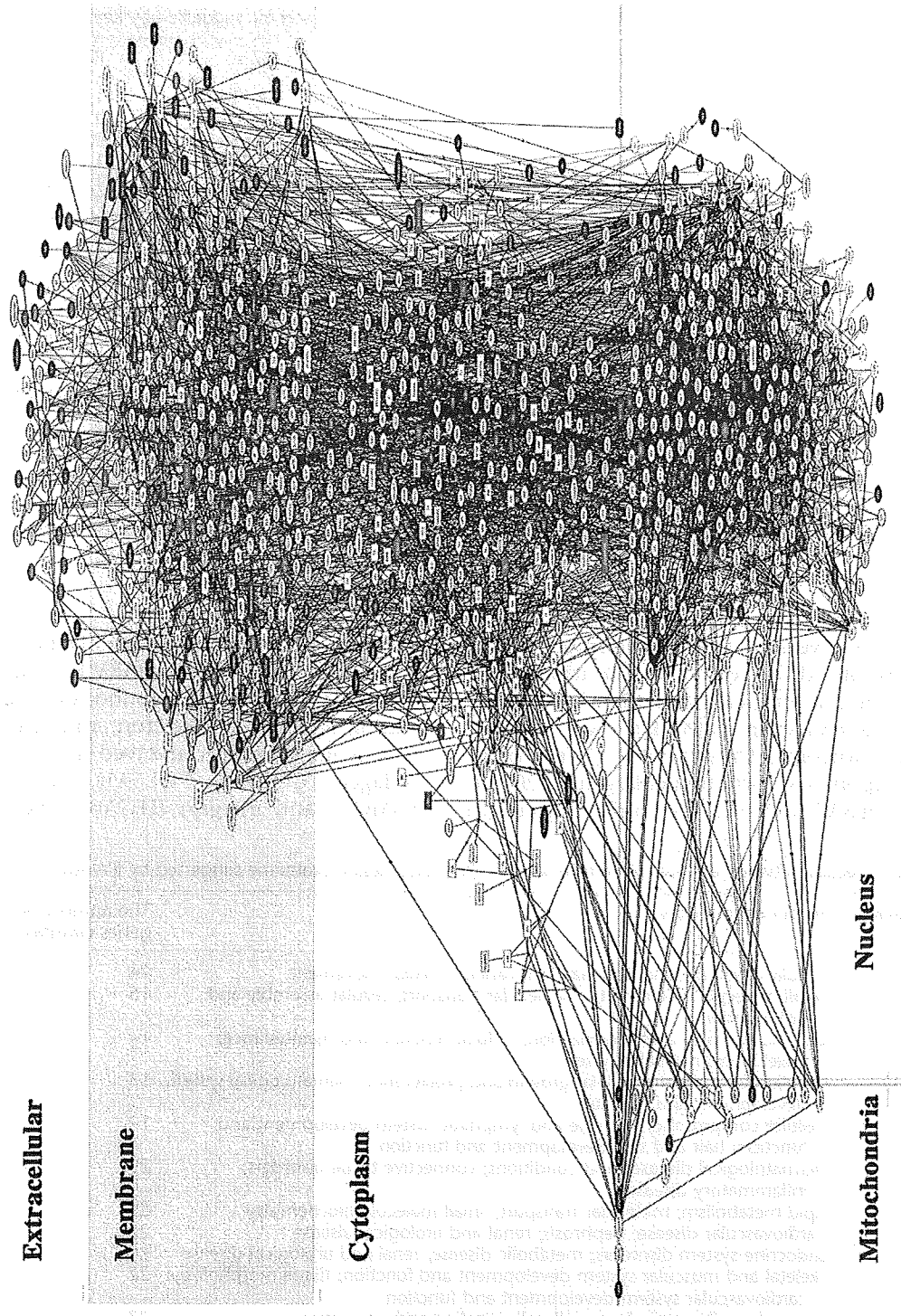

Figure 2 The molecular network of the CAP proteome suggested by KeyMolnet. The list of Entrez Gene IDs of CAP-specific proteome was uploaded onto the 'N-points to N-points search' tool of KeyMolnet. This generated a complex network composed of 1,120 fundamental nodes with 2,772 molecular relations, constructed by the shortest route connecting the start point of 75 MS-linked molecules of the KeyMolnet library (Supplementary Table 4)* and the end point of the CAP-specific proteome. The network is illustrated with respect to subcellular location of molecules. Red nodes represent start point molecules, whereas blue nodes represent end point molecules. Purple nodes express characteristics of both start and end point molecules. White nodes exhibit additional molecules extracted automatically from KeyMolnet core contents to establish molecular connections. The molecular relation is indicated by solid line with arrow (direct binding or activation), solid line with arrow and stop (direct inactivation), solid line without arrow (complex formation), dash line with arrow (transcriptional activation), and dash line with arrow and stop (transcriptional repression). *Supplementary Tables 1–4 are available online at http://msj.sagepub.com/

Table 3 The molecular network relevant to multiple sclerosis (MS) brain-lesion proteome suggested by KeyMolnet search

Stage	Rank	Functional category	Score	*P*-value
AP	1	IL-4 signaling pathway	42,324	1,794E-13
	2	IL-6 signaling pathway	40,966	4,656E-13
	3	IL-2 signaling pathway	36,684	9,059E-12
	4	Transcriptional regulation by STAT	32,789	1,347E-10
	5	Catenin signaling pathway	32,725	1,408E-10
CAP	1	PI3K signaling pathway	56,937	7,25E-18
	2	IL-4 signaling pathway	46,914	7,541E-15
	3	Transcriptional regulation by STAT	43,694	7,025E-14
	4	IFNα/βsignaling pathway	41,557	3,09E-13
	5	IL-6 signaling pathway	41,274	3,762E-13
CP	1	IL-4 signaling pathway	53,096	1,039E-16
	2	HGF signaling pathway	45,735	1,708E-14
	3	TCRα/βsignaling pathway	43,621	7,39E-14
	4	Integrin signaling pathway	38,501	2,572E-12
	5	IL-6 signaling pathway	38,115	3,359E-12

The list of Entrez Gene IDs of MS brain-lesion proteome was uploaded onto the 'N-points to N-points search' tool of KeyMolnet. The molecular network is constructed by the shortest route connecting the start point of 75 MS-related molecules of the KeyMolnet library (Supplementary Table 4) and the end point of MS lesion–specific proteome. Top 5 networks relevant to the proteome data are shown with the score and *P*-value.
Abbreviations: AP, acute plaques; CAP, chronic active plaques; CP, chronic plaques; PI3K, phosphoinositide-3-kinase; and HGF, hepatocyte growth factor.

immune cells, act as an adhesion receptor for cell trafficking and serve as a scaffold for immunological synapses. By the KEGG search, we identified focal adhesion, cell communication, and ECM-receptor interaction as molecular pathways most relevant to the CAP proteome. They involve a wide range of ECM components, including collagen (COL1A1, COL1A2, COL5A2, COL6A2, COL6A3), fibronectin (FN1), laminin (LAMA1), vitronectin (VTN), heparan sulfate proteoglycan (HSPG2), thrombospondin (THBS1), parvin (PARVA), and osteopontin (SPP1). Furthermore, we found focal adhesion, regulation of actin cytoskeleton, and cell communication as the pathways involved in CP. They include collagen (COL4A2, COL6A1), laminin (LAMB2, LAMC1), and integrin (ITGA6). The relevance of

Table 4 The molecular network relevant to multiple sclerosis (MS) brain-lesion proteome suggested by IPA search

Stage	Rank	Functional category	The number of genes classified	*P*-value
AP	1	Cellular assembly and organization; cancer; cellular movement	24	1,00E-49
	2	Small molecule biochemistry; molecular transport; cellular assembly and organization	15	1,00E-26
	3	Cellular assembly and organization; cellular function and maintenance; skeletal and muscular system	14	1,00E-24
	4	Cellular development; cellular growth and proliferation; hematological system development and function	13	1,00E-22
	5	Cellular compromise; immune and lymphatic system development and function; hair and skin development and function	12	1,00E-19
CAP	1	Dermatological diseases and conditions; connective tissue disorders; inflammatory disease	29	1,00E-47
	2	Lipid metabolism; molecular transport; small molecule biochemistry	29	1,00E-47
	3	Cardiovascular disease; nephrosis; renal and urological disease	25	1,00E-38
	4	Endocrine system disorders; metabolic disease; renal and urological disease	25	1,00E-38
	5	Skeletal and muscular system development and function; tissue morphology; cardiovascular system development and function	22	1,00E-31
CP	1	Cell cycle; cell morphology; cell–cell signaling and interaction	27	1,00E-50
	2	Tissue morphology; cardiovascular disease; cellular development	24	1,00E-43
	3	Cellular assembly and organization; cell morphology; cellular movement	22	1,00E-38
	4	Cellular assembly and organization; cellular development; cellular growth and proliferation	18	1,00E-29
	5	Cell–cell signaling and interaction, Hematological system development and function; Immune and lymphatic system development and function	15	1,00E-22

The list of Entrez Gene IDs of MS brain-lesion proteome was uploaded onto the 'Core Analysis' tool of IPA. Top five molecular networks relevant to the proteome data are shown with the number of genes classified and the score *P*-value.
Abbreviations: AP, acute plaques; CAP, chronic active plaques; and CP, chronic plaques.

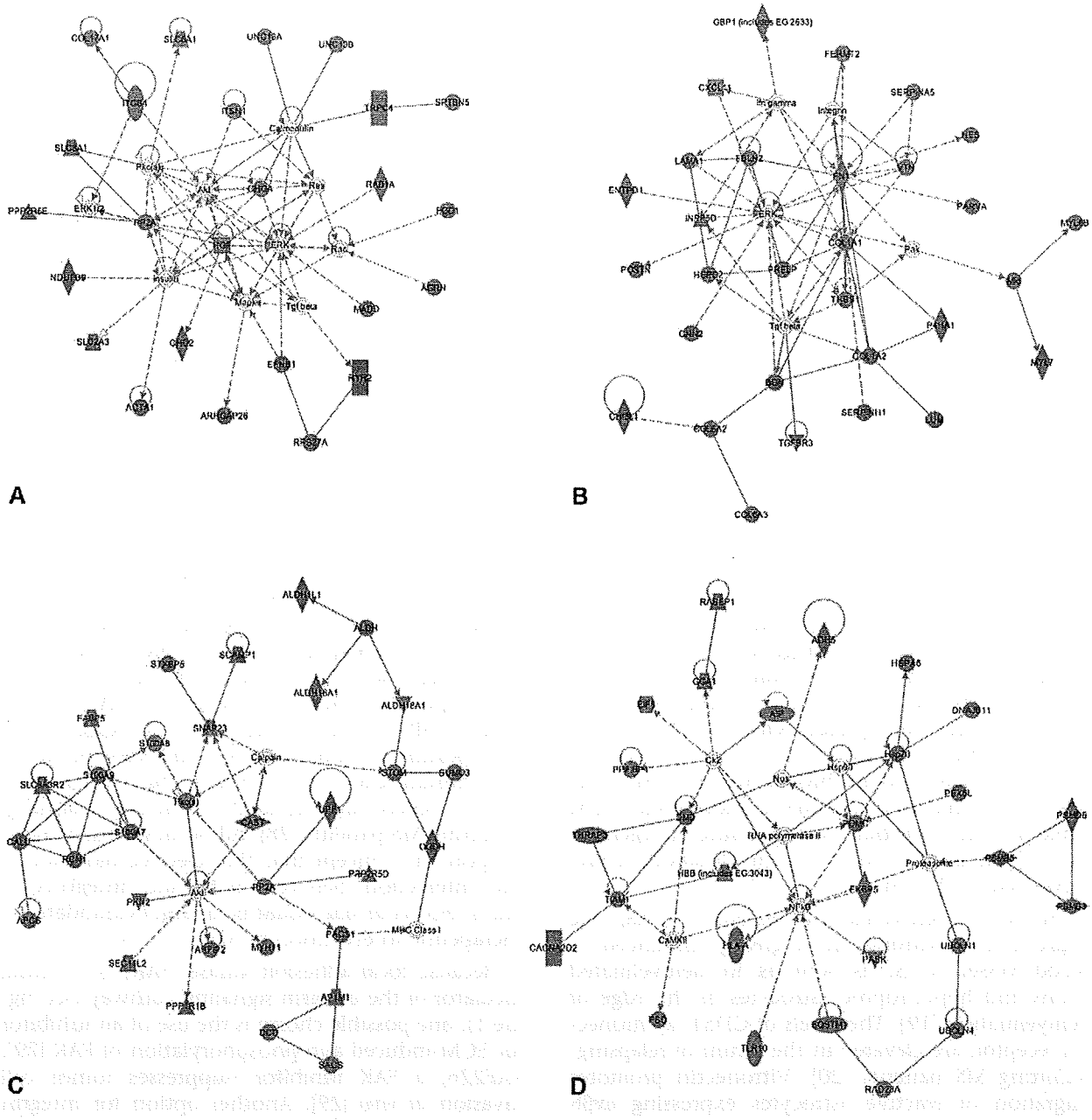

Figure 3 The molecular network of the AP, CAP, and CP proteome suggested by IPA. The list of Entrez Gene IDs of the MS lesion-specific proteome was uploaded onto the 'Core Analysis' tool of Ingenuity pathway analysis (IPA). Molecular networks most relevant to the AP (A), CAP (B and C), or CP (D) proteome are shown. Red nodes represent the molecules included in the gene list (Supplementary Tables 1–3). The molecular network (A) is constructed by 35 nodes, including ACTA1, AGRN, Akt, ARHGAP26, Calmodulin, CHD2, CHGA, COL17A1, EFNB1, ERK, ERK1/2, FGD1, HGF, insulin, ITGB4, ITSN1, MADD, Mapk, NDUFB9, Pkc(s), PP2A, PPP2R5E, RAB1A, Rac, Ras, RPS27A, RYR2, SLC2A3, SLC6A1, SLC8A1, SPTBN5, TGF-β, TRPC4, UNC13A, and UNC13B. The network (B) is constructed by 35 nodes, including BGN, CHI3L1, CNN2, COL1A1, COL1A2, COL6A2, COL6A3, CXCL11, ENTPD1, ERK, FBLN2, FERMT2, FN1, GBP1, HSPG2, IFN-γ, INPP5D, Integrin, LAMA1, LUM, Mlc, MYL7, MYL6B, NES, P4HA1, Pak, PARVA, POSTN, PRELP, SERPINA5, SERPINH1, TGF-β, TGFBR3, THBS1, and VTN. The network (C) is constructed by 35 nodes, including Akt, ALDH, ALDH16A1, ALDH18A1, ALDH1L1, AP1M1, APCS, ARFIP2, Calpain, CALU, CAST, DCD, FABP5, MHC Class I, MYH11, OGDH, PACS1, Pkc(s), PKN2, PP2A, PPP1R1B, PPP2R5D, RCN1, S100A7, S100A8, S100A9, SACS, SCAMP1, SEC14L2, SLC9A3R2, SNAP23, STOM, STXBP5, SUMO3, and UPF1. The network (D) is constructed by 35 nodes, including ADH5, AIP, CACNA2D2, CaMKII, Ck2, DMD, DNAJB11, EIF5, FKBP5, GGA1, HBB, HLA-A, Hsp70, Hsp90, HSPA6, NFkB, Nos, PASK, PEX5L, POMC, PPFIBP1, Proteasome, PSD, PSMB3, PSMB5, PSMD6, RABEP1, RAD23A, RNA polymerase II, SQSTM1, THRAP3, TIAM1, TLR10, UBQLN1, and UBQLN4. The molecular relation is indicated by solid line (direct interaction), dash line (indirect interaction), with filled arrow (acts on), stop (inhibits), stop and filled arrow (inhibits and acts on), and open arrow (translocates to).

Table 5 The molecular pathway relevant to MS brain-lesion proteome suggested by Ingenuity pathway analysis (IPA) search

Stage	Rank	Functional category	The number of genes classified	*P*-value
AP	1	Calcium signaling	7	2,53E-03
	2	Oxidative phosphorylation	4	2,69E-02
CAP	1	Calcium signaling	14	5,14E-04
	2	Hepatic fibrosis and hepatic stellate cell activation	11	1,53E-03
	3	Purine metabolism	16	3,05E-03
	4	Actin cytoskeleton signaling	13	5,77E-03
	5	Oxidative phosphorylation	9	1,12E-02
CP	1	Biosynthesis of steroids	4	7,37E-04
	2	Actin cytoskeleton signaling	8	8,00E-03
	3	Ubiquinone biosynthesis	4	9,54E-03
	4	Axonal guidance signaling	11	1,37E-02
	5	Integrin signaling	7	2,19E-02

The list of Entrez Gene IDs of MS brain-lesion proteome was uploaded onto the 'Core Analysis' tool of IPA. The canonical pathways relevant to the proteome data are shown with the number of genes classified and *P*-value.
Abbreviations: AP, acute plaques; CAP, chronic active plaques; and CP, chronic plaques.

the ECM and integrin signaling pathway to CAP and CP was further verified by molecular network analysis using PANTHER, KeyMolnet, and IPA followed by statistical evaluation. These *in silico* observations agree well with *in-vivo* studies, showing remarkable upregulation of diverse ECM constituents in MS brain lesions, where cytokine/chemokine-activated microglia, astrocytes, and infiltrating macrophages release a large amount of proteolytic enzymes bound to ECM molecules, which mediate myelin breakdown [17,18]. Glial scars in chronic lesions of MS include certain ECM proteins that contribute to the failure of regeneration of damaged axons and remyelination of preserved axons [17,18].

In active demyelinating lesions of MS, the expression of vitronectin is greatly enhanced in blood vessel walls, as well as in demyelinated axons and hypertrophic astrocytes at the edge of demyelination [19]. The levels of CD51, a vitronectin receptor, are elevated in the serum of relapsing-remitting MS patients [20]. Vitronectin promotes migration of reactive astrocytes expressing αvβ8 integrin [21]. In active demyelinating lesions of MS, fibronectin is accumulated in the brain parenchyma and is deposited abundantly in blood vessel walls and perivascular infiltrates [22]. Fibronectin facilitates migration of immune cells, promotes proliferation of astrocytes, and inhibits differentiation of oligodendrocyte progenitors [23]. In MS lesions, both vitronectin and fibronectin are derived mainly form plasma protein components passing across the disrupted blood–brain barrier and partly from the local synthesis by endothelial cells, macrophages, astrocytes, and infiltrating immune cells. Vitronectin and fibronectin activate microglia and upregulate MMP-9 production [24]. Thrombospondin produced by reactive astrocytes facilitates macrophage-mediated phagocytosis of apoptotic cells and possible uptake of degraded myelin via the ECM receptors CD36 and αvβ3 integrin [25]. Large-scale sequencing of MS plaque cDNA libraries showed that osteopontin (SPP1), a proinflammatory component of ECM, is one of the most abundant transcripts [26]. The clinical severity of EAE is attenuated in SPP1-deficient mice [26]. The expression of osteopontin is enhanced in astrocytes in active demyelinating lesions of MS [27]. The plasma osteopontin levels are elevated in active relapsing-remitting MS patients [28]. All of these observations support the concept that the selective blockade of the interaction between ECM and integrins in brain lesions *in situ* would be a target candidate for therapeutic intervention in MS.

Because focal adhesion kinase (FAK) is a central mediator of the integrin signaling pathway (see Figure 1), one possible choice is the use of an inhibitor for ECM-induced autophosphorylation of FAK [29]. TAE226, a FAK inhibitor, suppresses tumor cell invasion *in vivo* [29]. Another option for integrin signaling inhibitors is disintegrins, a group of small disulfide-rich peptides containing the arginine–glycine–aspartic acid sequence that mediates the selective binding to integrins [30]. Liposomal delivery of contortrostatin, a snake venome disintegrin, shows a tumor-suppressive anti-angiogenic activity [30]. However, a complete blockade of general function of integrins has a risk for inducing serious side effects [31]. Even in the context of the selective blockade, treatment with a humanized monoclonal antibody against VLA4, α4β1 integrin (natalizumab) reduced relapses 66% in clinical trials of MS but also activated the lethal infection of JC virus in some patients [32].

Acknowledgments

This work was supported by grants to J-IS from Research on Psychiatric and Neurological Diseases and Mental Health, the Ministry of Health, Labour and Welfare of Japan (H17-020), Research on Health Sciences Focusing on Drug Innovation, the Japan Health Sciences Foundation (KH21101), the Grant-in-Aid for Scientific Research, the Ministry of Education, Culture, Sports, Science and Technology, Japan (MEXT) (B18300118), the High-Tech Research Center Project, MEXT (S0801043) and from the Nakatomi Foundation.

References

1. Lassmann, H, Brück, W, Lucchinetti, CF. The immunopathology of multiple sclerosis: an overview. *Brain Pathol* 2007; **17**: 210–218.
2. Kieseier, BC, Wiendl, H, Hemmer, B, Hartung, HP. Treatment and treatment trials in multiple sclerosis. *Curr Opin Neurol* 2007; **20**: 286–293.
3. Kingsmore, SF, Lindquist, IE, Mudge, J, Gessler, DD, Beavis, WD. Genome-wide association studies: progress and potential for drug discovery and development. *Nat Rev Drug Discov* 2008; **7**: 221–230.
4. Steinman, L, Zamvil, S. Transcriptional analysis of targets in multiple sclerosis. *Nat Rev Immunol* 2003; **3**: 483–492.
5. Quintana, FJ, Farez, MF, Weiner, HL. Systems biology approaches for the study of multiple sclerosis. *J Cell Mol Med* 2008; doi 10.1111/j.1582-4934.2008.00375.x.
6. Lock, C, Hermans, G, Pedotti, R, *et al.* Gene-microarray analysis of multiple sclerosis lesions yields new targets validated in autoimmune encephalomyelitis. *Nat Med* 2002; **8**: 500–508.
7. Satoh, J, Nakanishi, M, Koike, F, *et al.* Microarray analysis identifies an aberrant expression of apoptosis and DNA damage-regulatory genes in multiple sclerosis. *Neurobiol Dis* 2005; **18**: 537–550.
8. Han, MH, Hwang, SI, Roy, DB, *et al.* Proteomic analysis of active multiple sclerosis lesions reveals therapeutic targets. *Nature* 2008; **451**: 1076–1081.
9. Ganter, B, Giroux, CN. Emerging applications of network and pathway analysis in drug discovery and development. *Curr Opin Drug Discov Devel* 2008; **11**: 86–94.
10. Viswanathan, GA, Seto, J, Patil, S, Nudelman, G, Sealfon, SC. Getting started in biological pathway construction and analysis. *PLoS Comput Biol* 2008; **4**: e16.
11. Albert, R, Jeong, H, Barabasi, AL. Error and attack tolerance of complex networks. *Nature* 2000; **406**: 378–382.
12. Kanehisa, M, Araki, M, Goto, S, *et al.* KEGG for linking genomes to life and the environment. *Nucleic Acids Res* 2008; **36**: D480–D484.
13. Mi, H, Guo, N, Kejariwal, A, Thomas, PD. PANTHER version 6: protein sequence and function evolution data with expanded representation of biological pathways. *Nucleic Acids Res* 2007; **35**: D247–D252.
14. Palacios, R, Goni, J, Martinez-Forero, I, *et al.* A network analysis of the human T-cell activation gene network identifies JAGGED1 as a therapeutic target for autoimmune diseases. *PLoS ONE* 2007; **2**: e1222.
15. Sato, H, Ishida, S, Toda, K, *et al.* New approaches to mechanism analysis for drug discovery using DNA microarray data combined with KeyMolnet. *Curr Drug Discov Technol* 2005; **2**: 89–98.
16. Luo, BH, Carman, CV, Springer, TA. Structural basis of integrin regulation and signaling. *Annu Rev Immunol* 2007; **25**: 619–647.
17. Sobel, RA. The extracellular matrix in multiple sclerosis lesions. *J Neuropathol Exp Neurol* 1998; **57**: 205–217.
18. van Horssen, J, Dijkstra, CD, de Vries, HE. The extracellular matrix in multiple sclerosis pathology. *J Neurochem* 2007; **103**: 1293–1301.
19. Sobel, RA, Chen, M, Maeda, A, Hinojoza, JR. Vitronectin and integrin vitronectin receptor localization in multiple sclerosis lesions. *J Neuropathol Exp Neurol* 1995; **54**: 202–213.
20. Minagar, A, Jy, W, Jimenez, JJ, *et al.* Elevated plasma endothelial microparticles in multiple sclerosis. *Neurology* 2001; **56**: 1319–1324.
21. Milner, R, Huang, X, Wu, J, *et al.* Distinct roles for astrocyte αvβ5 and αvβ8 integrins in adhesion and migration. *J Cell Sci* 1999; **112**: 4271–4279.
22. Sobel, RA, Mitchell, ME. Fibronectin in multiple sclerosis lesions. *Am J Pathol* 1989; **135**: 161–168.
23. Sisková, Z, Baron, W, de Vries, H, Hoekstra, D. Fibronectin impedes "myelin" sheet-directed flow in oligodendrocytes: a role for a beta 1 integrin-mediated PKC signaling pathway in vesicular trafficking. *Mol Cell Neurosci* 2006; **33**: 150–159.
24. Milner, R, Crocker, SJ, Hung, S, Wang, X, Frausto, RF, del Zoppo, GJ. Fibronectin- and vitronectin-induced microglial activation and matrix metalloproteinase-9 expression is mediated by integrins $\alpha_5\beta_1$ and $\alpha_v\beta_5$. *J Immunol* 2007; **178**: 8158–8167.
25. Ren, Y, Savill, J. Proinflammatory cytokines potentiate thrombospondin-mediated phagocytosis of neutrophils undergoing apoptosis. *J Immunol* 1995; **154**: 2366–2374.
26. Chabas, D, Baranzini, SE, Mitchell, D, *et al.* The influence of the proinflammatory cytokine, osteopontin, on autoimmune demyelinating disease. *Science* 2001; **294**: 1731–1735.
27. Sinclair, C, Kirk, J, Herron, B, Fitzgerald, U, McQuaid, S. Absence of aquaporin-4 expression in lesions of neuromyelitis optica but increased expression in multiple sclerosis lesions and normal-appearing white matter. *Acta Neuropathol* 2007; **113**: 187–194.
28. Vogt, MH, Lopatinskaya, L, Smits, M, Polman, CH, Nagelkerken, L. Elevated osteopontin levels in active relapsing-remitting multiple sclerosis. *Ann Neurol* 2003; **53**: 819–822.
29. Liu, TJ, LaFortune, T, Honda, T, *et al.* Inhibition of both focal adhesion kinase and insulin-like growth factor-I receptor kinase suppresses glioma proliferation *in vitro* and *in vivo*. *Mol Cancer Ther* 2007; **6**: 1357–1367.
30. Swenson, S, Costa, F, Minea, R, *et al.* Intravenous liposomal delivery of the snake venom disintegrin contortrostatin limits breast cancer progression. *Mol Cancer Ther* 2004; **3**: 499–511.
31. Cantor, JM, Ginsberg, MH, Rose, DM. Integrin-associated proteins as potential therapeutic targets. *Immunol Rev* 2008; **223**: 236–251.
32. Steinman, L. Blocking adhesion molecules as therapy for multiple sclerosis: natalizumab. *Nat Rev Drug Discov* 2005; **4**: 510–518.

Cell Mol Neurobiol (2009) 29:423–438
DOI 10.1007/s10571-008-9338-2

ORIGINAL PAPER

Gene Expression Profiling of Human Neural Progenitor Cells Following the Serum-Induced Astrocyte Differentiation

Shinya Obayashi · Hiroko Tabunoki · Seung U. Kim · Jun-ichi Satoh

Received: 16 August 2008 / Accepted: 10 December 2008 / Published online: 7 January 2009

Abstract Neural stem cells (NSC) with self-renewal and multipotent properties could provide an ideal cell source for transplantation to treat spinal cord injury, stroke, and neurodegenerative diseases. However, the majority of transplanted NSC and neural progenitor cells (NPC) differentiate into astrocytes in vivo under pathological environments in the central nervous system, which potentially cause reactive gliosis. Because the serum is a potent inducer of astrocyte differentiation of rodent NPC in culture, we studied the effect of the serum on gene expression profile of cultured human NPC to identify the gene signature of astrocyte differentiation of human NPC. Human NPC spheres maintained in the serum-free culture medium were exposed to 10% fetal bovine serum (FBS) for 72 h, and processed for analyzing on a Whole Human Genome Microarray of 41,000 genes, and the microarray data were validated by real-time RT-PCR. The serum elevated the levels of expression of 45 genes, including ID1, ID2, ID3, CTGF, TGFA, METRN, GFAP, CRYAB and CSPG3, whereas it reduced the expression of 23 genes, such as DLL1, DLL3, PDGFRA, SOX4, CSPG4, GAS1 and HES5. Thus, the serum-induced astrocyte differentiation of human NPC is characterized by a counteraction of ID family genes on Delta family genes. Coimmunoprecipitation analysis identified ID1 as a direct binding partner of a proneural basic helix-loop-helix (bHLH) transcription factor MASH1. Luciferase assay indicated that activation of the DLL1 promoter by MASH1 was counteracted by ID1. Bone morphogenetic protein 4 (BMP4) elevated the levels of ID1 and GFAP expression in NPC under the serum-free culture conditions. Because the serum contains BMP4, these results suggest that the serum factor(s), most probably BMP4, induces astrocyte differentiation by upregulating the expression of ID family genes that repress the proneural bHLH protein-mediated Delta expression in human NPC.

Keywords Astrocytes · Delta family genes · Human neuronal progenitor cells · ID family genes · Microarray

Abbreviations

NSC	Neural stem cells
NPC	Neural progenitor cells
CNS	Central nervous system
BBB	Blood–brain barrier
bHLH	Basic helix-loop-helix
FBS	Fetal bovine serum
EGF	Epidermal growth factor
bFGF	Basic fibroblast growth factor
LIF	Leukemia inhibitory factor
TGF	Transforming growth factor
RT-PCR	Reverse transcription-polymerase chain reaction
DAVID	Database for annotation visualization and integrated discovery
GO	Gene Ontology
GFAP	Glial fibrillary acidic protein
BMP4	Bone morphogenetic protein 4

S. Obayashi · H. Tabunoki · J.-i. Satoh (✉)
Department of Bioinformatics and Molecular Neuropathology, Meiji Pharmaceutical University, 2-522-1 Noshio, Kiyose, Tokyo 204-8588, Japan
e-mail: satoj@my-pharm.ac.jp

S. U. Kim
Division of Neurology, Department of Medicine, University of British Columbia Hospital, University of British Columbia, Vancouver, BC, Canada

Introduction

Neural stem cells (NSC) with self-renewal and multipotent properties are distributed broadly in the niche of germinal zones in the embryonic and adult mammalian central nervous system (CNS). NSC, unlimitedly propagated in vitro and genetically manipulated ex vivo, could provide an ideal cell source for transplantation to compensate for cell damage in spinal cord injury, stroke, and neurodegenerative diseases (Martino and Pluchino 2006). However, the majority of transplanted NSC and neural progenitor cells (NPC), the cells committed to differentiation into the neuronal lineage, differentiate into astrocytes in vivo under pathological environments in the CNS, which contribute to glial scar formation that inhibits axonal regeneration (Pallini et al. 2005; Ishii et al. 2006). Oxidative stress mediators abundant in pathological lesions elevate the expression of histone deacethylase (HDAC) Sirt1 in mouse NPC, which cooperates with an inhibitory basic helix-loop-helix (bHLH) protein HES1 to mediate epigenetic silencing of a proneural bHLH transcription factor MASH1, leading to astrocyte differentiation of NPC (Prozorovski et al. 2008). To obtain a subset of neurons desirable for cell replacement therapy for human neurological diseases, we should intensively clarify the complex interaction of intrinsic genetic programs and environmental factors that regulate human NSC and NPC proliferation and differentiation. However, at present, molecular mechanisms underlying astrocytic differentiation of human NSC and NPC in vitro and in vivo remain largely unknown.

DNA microarray technology is a powerful approach that allows us to systematically monitor gene expression profile of neural cells during differentiation under development. Microarray analysis showed that neuronal differentiation of human NSC in culture involves the regulation of hundreds of genes, including those essential for Wnt and TGF-beta signaling pathways (Cai et al. 2006). By comparing gene expression profiles between human NPC and differentiated neurons, a previous study identified both PDGF receptor alpha (PDGFRA) and IGF-binding protein 4 (IGFBP4) as key proneural differentiation factors (Yu et al. 2006). A recent study discovered 38 genes expressed commonly between adult and fetal human NPC (Maisel et al. 2007). Recently, we have characterized the DNA damage-responsive gene signature of human astrocytes in culture (Satoh et al. 2006).

Because the serum is a potent inducer of astrocyte differentiation of rodent NSC and NPC in culture (Chiang et al. 1996; Brunet et al. 2004), and the serum components enter the CNS via the disrupted blood–brain barrier (BBB) at the site of CNS injury and ischemia, we studied the effect of the serum on gene expression profile of human NPC in culture by analyzing with a whole genome-scale microarray to identify the gene signature of astrocyte differentiation of human NPC.

Methods

Neural Progenitor Cells in Culture

Cryopreserved human NPC, isolated from the brain of an 18.5-week-old female Caucasian under informed consent, were obtained from Cambrex (Walkersville, MD, USA) as a commercially available product (CC-2599). NPC were plated in a 6-well culture plate coated with polyethyleneimine, and incubated at 37°C in a 5% CO_2/95% air incubator in the NPC medium, composed of the serum-free DMEM/F-12 medium (Invitrogen, Carlsbad, CA, USA) supplemented with a mixture of insulin–transferrin–selenium (ITS) (Invitrogen), 20 ng/ml recombinant human EGF (Higeta, Tokyo, Japan), 20 ng/ml recombinant human bFGF (PeproTech EC, London, UK), and 10 ng/ml recombinant human LIF (Chemicon, Temecula, CA, USA), according to the methods described previously (Carpenter et al. 1999). The half of the medium was renewed every 4 days. Following incubation for several months, NPC in culture continued to proliferate by forming free floating or loosely attached growing spheres. For microarray analysis, nonpassage NPC spheres were harvested, replated in a non-coated 6-well culture plate, and incubated further for 72 h in the NPC medium with or without inclusion of 10% fetal bovine serum (FBS) (Biowest, Miami, FL, USA). In some experiments, NPC were incubated for 72 h in the NPC medium with or without inclusion of 50 ng/ml recombinant human BMP4 (PeproTech).

Human cell lines, such as NTera2 teratocarcinoma, Y79 retinoblastoma, SK-N-SH neuroblastoma, IMR-32 neuroblastoma, U-373MG astrocytoma, HMO6 microglia, HeLa cervical carcinoma, and HepG2 hepatoblastoma, were maintained as described previously (Satoh et al. 2007).

Gene Expression Profiling

Five micrograms of total RNA was isolated from NPC cells by using TRIZOL reagent (Invitrogen). It was in vitro amplified once, and cRNA was processed for microarray analysis on a Whole Human Genome Oligonucleotide Microarray (G4112A, 41,000 genes; Agilent Technologies, Palo Alto, CA, USA), as described previously (Satoh et al. 2006). cRNA prepared from NPC spheres without exposure to the serum (S−) was labeled with a fluorescent dye Cy3, while cRNA of NPC spheres with exposure to the serum (S+) was labeled with Cy5. The array was hybridized at

60°C for 17 h in the hybridization buffer containing equal amounts of Cy3- or Cy5-labeled cRNA. Then, it was scanned by the Agilent scanner (Agilent Technologies). The data were analyzed by using the Feature Extraction software (Agilent Technologies). The fluorescence intensities (FI) of individual spots were quantified following global normalization between Cy3 and Cy5 signals and subsequent Lowess normalization. The ratio of FI of Cy5 signal versus FI of Cy3 signal exceeding 2.0 was defined as significant upregulation, whereas the ratio smaller than 0.5 was considered as substantial downregulation.

Real-Time RT-PCR Analysis

DNase-treated total cellular RNA was processed for cDNA synthesis using oligo(dT)$_{12-18}$ primers and SuperScript II reverse transcriptase (Invitrogen). Then, cDNA was amplified by PCR in LightCycler ST300 (Roche Diagnostics, Tokyo, Japan) using SYBR Green I and primer sets listed in Table 1. The expression levels of target genes were standardized against those of the glyceraldehyde-3-phosphate dehydrogenase (G3PDH) gene detected in parallel in identical cDNA samples. All the assays were performed in triplicate.

Functional Annotation and Molecular Network Analysis

Functional annotation of significant genes identified by microarray analysis was searched by the web-accessible program named Database for Annotation, Visualization and Integrated Discovery (DAVID) version 2008, National Institute of Allergy and Infectious Diseases (NIAID), National Institutes of Health (NIH) (david.abcc.ncifcrf.gov) (Dennis et al. 2003). DAVID covers more than 40 annotation categories, including Gene Ontology (GO) terms, protein–protein interactions, protein functional domains, disease associations, biological pathways, sequence general features, homologies, gene functional summaries, and tissue expressions. By importing the list of the National Center for Biotechnology Information (NCBI) Entrez Gene IDs, this program creates the functional annotation chart, an annotation-term-focused view that lists annotation terms and their associated genes under study. To avoid excessive count of duplicated genes, the Fisher's exact test is calculated based on corresponding DAVID gene IDs by which all redundancies in original IDs are removed.

KeyMolnet is a knowledge-based content database that focuses on relationships among human genes, molecules, diseases, pathways and drugs, which were manually curated by expert biologists (www.immd.co.jp/en/keymolnet/index.html) (Sato et al. 2005). They are categorized into the core contents collected from selected review articles with the highest reliability or the secondary contents extracted from abstracts of PubMed database. The "N-points to N-points" network-search algorithm identifies the molecular network constructed by the shortest route connecting the start point molecules and the end point molecules. The generated network was compared side by side with 346 human canonical pathways of the KeyMolnet library. The algorithm counting the number of overlapping molecular relations between the extracted network and the canonical pathway makes it possible to identify the canonical pathway showing the statistically significant contribution to the extracted network.

Immunohistochemistry

For immunocytochemistry, NPC attached on poly-L-lysine-coated cover glasses were fixed with 4% PFA in 0.1 M phosphate buffer, pH 7.4 at room temperature (RT) for 5 min, followed by incubation with phosphate-buffered saline (PBS) containing 0.5% Triton X-100 at RT for 3 min. After blocking non-specific staining by PBS containing 10% NGS, the cells were incubated at RT for 30 min with a mixture of mouse monoclonal anti-GFAP antibody (GA5; Nichirei, Tokyo, Japan) and rabbit polyclonal anti-nestin antibody (AB5922; Chemicon) or rabbit polyclonal anti-ID1 antibody (C-20; Santa Cruz Biotechnology, Santa Cruz, CA, USA). Then, they were incubated at RT for 30 min with a mixture of Alexa Fluor 488-conjugated anti-rabbit IgG (Invitrogen) and Alexa Fluor 568-conjugated anti-mouse IgG (Invitrogen). After several washes, they were examined on the Olympus BX51 universal microscope.

Western Blot Analysis

To prepare total protein extract, the cells were homogenized in RIPA buffer containing and a cocktail of protease inhibitors (Sigma, St. Louis, MO, USA). Following centrifugation at 12,000 rpm for 10 min at RT, the supernatant was collected and separated on a 12% or 15% SDS–PAGE gel. After gel electrophoresis, the protein was transferred onto nitrocellulose membranes, and the blots were labeled at RT overnight with anti-GFAP antibody (GA5) or anti-ID1 antibody (C-20). Then, they were incubated at RT for 30 min with HRP-conjugated anti-mouse or rabbit IgG (Santa Cruz Biotechnology). The specific reaction was visualized by exposing to a chemiluminescence substrate (Pierce, Rockford, IL, USA). After the antibodies were stripped by incubating the membranes at 50°C for 30 min in stripping buffer, composed of 62.5 mM Tris-HCl, pH 6.7, 2% SDS and 100 mM 2-mercaptoethanol, the blots were processed for relabeling with anti-HSP60 antibody (N-20; Santa Cruz Biotechnology).

Table 1 Primers for PCR for RT-PCR and cloning utilized in the present study

Genes	GenBank accession No.	Sense primers	Antisense primers	Application
NES	NM_006617	5′ctgctcaggagcagcactcttaac3′	5′cttagcctatgagatggagcaggc3′	Real-time RT-PCR
MSI1	NM_002442	5′caaagtgtctatctgggtgtgggc3′	5′acagctgaggcctgcaagcttaca3′	Real-time RT-PCR
GFAP	NM_002055	5′atgaggaggaaggagagaagggga3′	5′ccttccctttcctgtctgagtctc3′	Real-time RT-PCR
NFH	NM_021076	5′gagaaaggaacatccggaacagcc3′	5′tgggagtgccctctcttgctaaca3′	RT-PCR
MBP	NM_002385	5′gttccggaatcctgtcctcagctt3′	5′taactgttggccggaaattgccgg3′	RT-PCR
ID1	NM_002165	5′aattacgtgctctgtgggtctccc3′	5′gtctctggtgactagtaggtgtgc3′	Real-time RT-PCR
ID1	NM_002165	5′atcatggaagtcgccagtggcagc3′	5′tcagcgacacaagatgcgatcgtc3′	Cloning for luciferase assay
Myc-tagged ID1	NM_002165	5′cggaattccgaaagtcgccagtggcagcac3′	5′gaagatcttctcagcgacacaagatgcgat3′	Cloning for CoIP assay
ID3	NM_002167	5′aacttcgccctgcccacttgactt3′	5′cacctccacgctctgaaaagacct3′	Real-time RT-PCR
NPTX1	NM_002522	5′ttgtcctcatgcacacgaagcagc3′	5′acacgcacacacagatcctctcac3′	Real-time RT-PCR
FOS	NM_005252	5′gagctggtgcattacagagaggag3′	5′ggacttgagtccacacatggatgc3′	Real-time RT-PCR
DLL1	NM_005618	5′acgaatgctgctgaagaggaggga3′	5′aactgtccatagtgcaacggcgac3′	Real-time RT-PCR
MASH1	NM_004316	5′tgagtaaggtggagacactgcgct3′	5′tcagaaccagttggtgaagtcgagaag3′	Real-time RT-PCR
Flag-tagged MASH1	NM_002165	5′cggaattccgaaagctctgccaagatggag3′	5′cgggatcccgtcagaaccagttggtgaagt3′	Cloning for CoIP assay and luciferase assay
G3PDH	NM_002046	5′ccatgttcgtcatgggtgtgaacca3′	5′gccagtagaggcagggatgatgttc3′	Real-time RT-PCR
DLL promoter #1	AF222310	5′ggggtacccctcctgacactaggtggcaaga3′	5′gaagatcttcctcggcctccctccgcctggt3′	Cloning for luciferase assay
DLL promoter #2	AF222310	5′ccgctcgagcggaccccctcggctgccgccgcgg3′	5′gaagatcttcggacagcgcggcggcggcgac3′	Cloning for luciferase assay

NES nestin, *MSI1* musashi homolog 1, *GFAP* glial fibrillary acidic protein, *NFH* neurofilament heavy polypeptide, *MBP* myelin basic protein, *ID1* inhibitor of DNA binding 1, *ID3* inhibitor of DNA binding 3, *NPTX1* neuronal pentraxin 1, *FOS* cellular oncogene c-fos, *DLL1* delta-like 1, *MASH1* mammalian achaete scute homolog 1, *G3PDH* glyceraldehyde-3-phosphate dehydrogenase, *CoIP* coimmunoprecipitation. The underlined sequences represent restriction enzyme sites

Coimmunoprecipitation Analysis

The open-reading frame (ORF) of the human ID1 and MASH1 (ASCL1) genes were amplified by PCR using PfuTurbo DNA polymerase (Stratagene, La Jolla, CA, USA) and primer sets listed in Table 1. They were then cloned into the mammalian expression vector pCMV-Myc (Clontech, Mountain View, CA, USA) or p3XFLAG-CMV7.1 (Sigma) to express a fusion protein with an N-terminal Myc or Flag tag. At 48 h after co-transfection of the vectors in HEK293 cells by Lipofectamine 2000 reagent (Invitrogen), the cells were homogenized in M-PER lysis buffer (Pierce) supplemented with a cocktail of protease inhibitors (Sigma). After preclearance, the supernatant was incubated at 4°C for 3 h with rabbit polyclonal anti-Myc-conjugated agarose (Sigma), mouse monoclonal anti-Flag M2 affinity gel (Sigma), or the same amount of normal mouse or rabbit IgG-conjugated agarose (Santa Cruz Biotechnology). After several washes, the immunoprecipitates were processed for Western blot analysis using rabbit polyclonal anti-Myc antibody (Sigma) and mouse monoclonal anti-FLAG M2 antibody (Sigma).

Dual Luciferase Assay

The ORF of the human ID1 gene, amplified by PCR using PfuTurbo DNA polymerase and primer sets listed in Table 1, was cloned into the mammalian expression vector pEF6/V5-His TOPO (Invitrogen) by designing omission of V5 and His tags. The web search on Database of Transcriptional Start Sites (DBTSS; dbtss.hgc.jp) indicated that several E-box (CANNTG) sequences were clustered in the approximately 3,000 bp promoter region of the human DLL1 gene. Two non-overlapping regions of the DLL1 promoter, consisting of the region #1 spanning −1,253 and −254 containing two E-box sequences or the region #2 spanning −2,946 and −1,786 containing 10 E-box sequences, when the first amino acid of the initiation codon is defined as the position zero, were separately amplified by PCR using GC-RICH PCR system (Roche Diagnostics) and primer sets listed in Table 1. They were then cloned into the Firefly luciferase reporter vector pGL4.14-luc2-Hygro (Promega, Madison, WI, USA). The Renilla luciferase reporter vector pGL4.74-hRluc-TK (Promega) was used for an internal control that normalizes variability caused by differences in transfection efficacy. They were co-transfected in HEK293 cells, which were introduced with MASH1 and/or ID1 expression vectors at 36 h before transfection of the luciferase reporter vectors. At 16 h after transfection of the luciferase reporter vectors, cell lysate was processed for dual luciferase assay on a 20/20 Luminometer (Promega). All the assays were performed in triplicate.

Results

Human Neural Progenitor Cells (NPC) in Culture

Human NPC were capable of proliferating for several months by forming free floating or loosely attached growing spheres, when incubated in the NPC medium under the serum-free culture conditions (Fig. 1a). When human NPC spheres were incubated in the NPC medium supplemented with 10% FBS, they rapidly attached on the plastic surface, followed by vigorous outgrowth of a sheet of adherent cells from the attachment face (Fig. 1b). By RT-PCR analysis, NPC cells expressed the transcripts of nestin (NES), musashi homolog 1 (MSI1), and GFAP at high levels, whereas they displayed fairly low levels of NFH and MBP mRNA under culture conditions with or without inclusion of the serum (Fig. 1c, lanes 1–10).

When incubated in the serum-free NPC medium, the great majority of the cells forming the core of NPC spheres exhibited an intense immunoreactivity for nestin, and expressed less intensely immunoreactivity for GFAP (Fig. 2a). In contrast, when incubated in the 10% FBS-containing NPC medium, virtually all of adherent cells with a polygonal shape, growing out from the NPC spheres, expressed very strongly both GFAP and nestin immunoreactivities (Fig. 2b and d–f). None of the cells expressed the oligodendrocyte marker O4 or O1 in the serum-free and serum-containing culture conditions (data not shown). These results suggest that adherent cells growing from NPC spheres at the attachment face represent the cells that underwent astrocyte differentiation.

Upregulated Genes in Human NPC Following Exposure to the Serum

NPC spheres were harvested, replated on a non-coated plastic surface, and incubated further for 72 h in the NPC medium with (S+) or without (S−) inclusion of 10% FBS. Then, total cellular RNA was processed for microarray analysis. Exposure of NPC spheres to the serum elevated the levels of expression of 45 genes (Table 2). They include tropomodulin 1 (TMOD1), inhibitor of DNA binding 1 (ID1), connective tissue growth factor (CTGF), Kruppel-like factor 9 (KLF9), inhibitor of DNA binding 3 (ID3), fibroblast growth factor binding protein 2 (FGFBP2), zinc finger protein 436 (ZNF436), transforming growth factor alpha (TGFA), tumor protein D52 (TPD52), sulfatase 1 (SULF1), regulator of G-protein signaling 4 (RGS4), collectin sub-family member 12 (COLEC12), angiotensinogen (AGT), solute carrier family 16, member 9 (SLC16A9), meteorin (METRN), cathepsin H (CTSH), growth arrest and DNA-damage-inducible beta (GADD 45B), sterile alpha motif domain containing 11 (SAMD11),

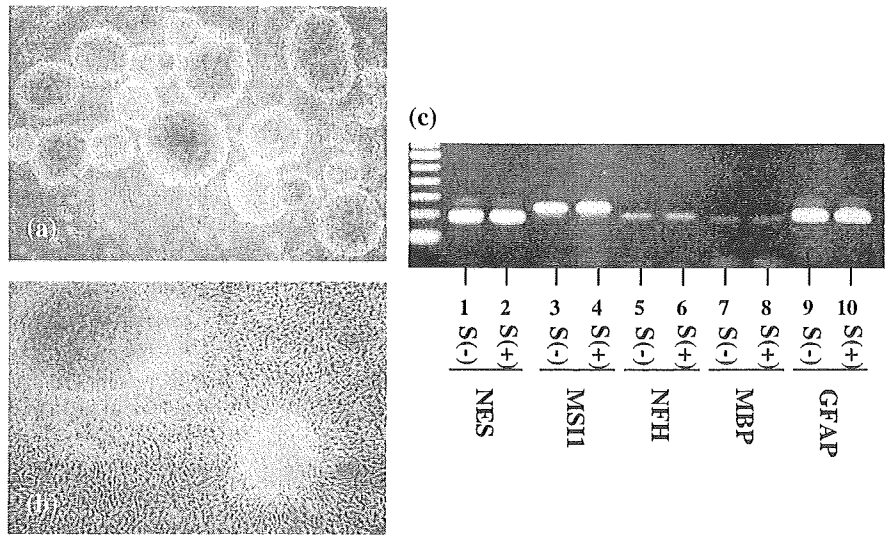

Fig. 1 Human neural progenitor cells (NPC) in culture. **a** Human NPC maintained under the serum-free culture conditions formed free floating growing spheres. **b** Human NPC spheres exposed to 10% FBS rapidly attached on the plastic surface, followed by vigorous outgrowth of a sheet of adherent cells from the attachment face. **a**, **b** Phase-contrast photomicrographs. **c** RT-PCR amplified for 32 cycles of nestin (NES, lanes 1 and 2), musashi homolog 1 (MSI1, lanes 3 and 4), neurofilament heavy polypeptide (NFH, lanes 4 and 6), myelin basic protein (MBP, lanes 7 and 8), and glial fibrillary acidic protein (GFAP, lanes 9 and 10) expressed in human NPC under the serum-free (S−) and the 10% FBS-containing (S+) culture conditions

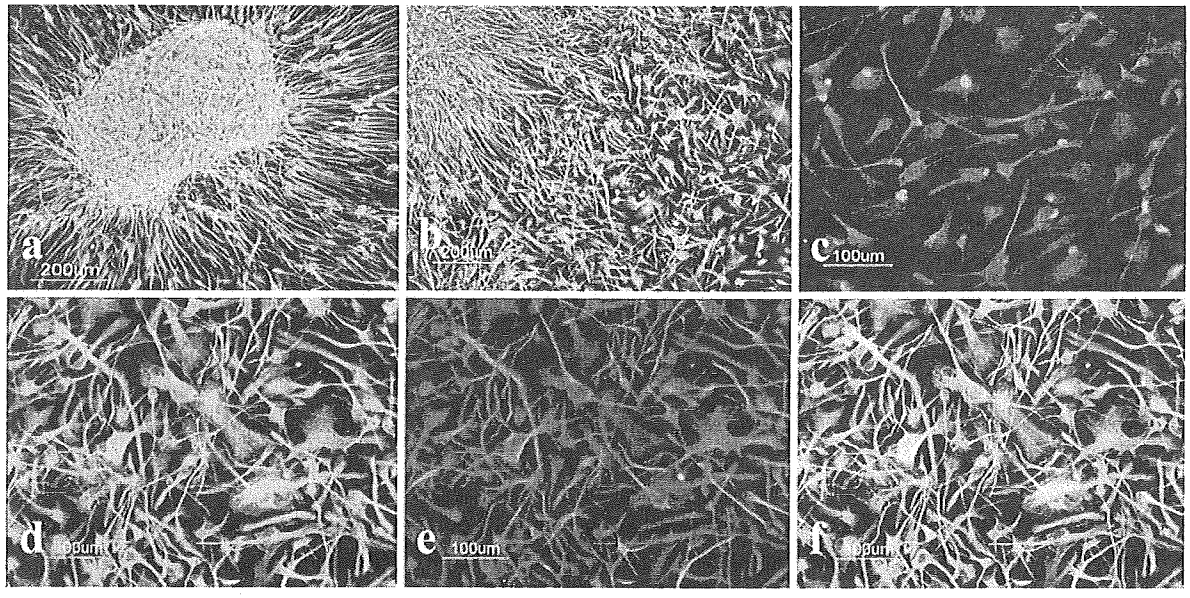

Fig. 2 Nestin, GFAP, and ID1 expression in human NPC in culture. Human NPC spheres attached on poly-L-lysine-coated cover glasses were incubated for 72 h in the NPC medium with (S+) or without (S−) inclusion of 10% FBS, and processed for double-labeling immunocytochemistry for nestin, GFAP, or ID1. **a** S−, NPC sphere, merge of nestin (green) and GFAP (red), **b** S+, vigorous outgrowth of adherent cells from the attachment face of the sphere, merge of nestin (green) and GFAP (red), **c** S+, outgrowth of adherent cells, merge of ID1 (green) and GFAP (red), **d** S+, outgrowth of adherent cells, nestin (green), **e** the same field as **d**, GFAP (red), and **f** merge of **d** and **e**

adenomatosis polyposis coli 2 (APC2), solute carrier family 2 member 5 (SLC2A5), GFAP, coiled-coil domain containing 103 (CCDC103), chromosome 9 open reading frame 58 (C9orf58), chitinase 3-like 2 (CHI3L2), complement factor I (CFI), chemokine C-X-C motif ligand 14 (CXCL14), annexin A1 (ANXA1), regulator of calcineurin 1 (RCAN1), retinal pigment epithelium-specific protein 65 kDa (RPE65), serine/threonine kinase 17a (STK17A), chromosome 4 open reading frame 30 (C4orf30), alpha B crystallin (CRYAB), transmembrane protein 132B (TMEM132B), frizzled homolog 1 (FZD1), inhibitor of DNA binding 2 (ID2), CDC42 effector protein 4

Table 2 Upregulated genes in human neuronal progenitor cells (NPC) following exposure to the serum

Rank	Gene symbol	Gene ID	Ratio	Gene name	Putative function
1	TMOD1	7111	13.05	Tropomodulin 1	A modulator of association between tropomyosin and the spectrin-actin complex
2	ID1	3397	9.00	Inhibitor of DNA binding 1, dominant negative helix-loop-helix protein	A HLH protein that acts as a dominant negative regulator of bHLH family transcription factors
3	CTGF	1490	5.17	Connective tissue growth factor	A secreted mitogenic protein with insulin-like growth factor-binding capacity
4	KLF9	687	4.43	Kruppel-like factor 9	A transcription factor that binds to GC box elements
5	ID3	3399	4.08	Inhibitor of DNA binding 3, dominant negative helix-loop-helix protein	A HLH protein that acts as a dominant negative regulator of bHLH family transcription factors
6	FGFBP2	83888	3.76	Fibroblast growth factor binding protein 2	A protein of unknown function secreted by T lymphocytes
7	ZNF436	80818	3.67	Zinc finger protein 436	A trancriptional factor that represses transcriptional activities of SRE and AP-1
8	TGFA	7039	3.60	Transforming growth factor, alpha	A growth factor that competes with EGF for binding to EGF receptor
9	TPD52	7163	3.35	Tumor protein D52	A coiled-coil domain bearing protein involved in calcium-mediated signal transduction and cell proliferation
10	SULF1	23213	3.23	Sulfatase 1	An endosulfatase that modulates signaling by heparin-binding growth factors
11	RGS4	5999	3.13	Regulator of G-protein signaling 4	A member of RGS family that deactivates G protein subunits of heterotrimeric G proteins
12	COLEC12	81035	2.93	Collectin sub-family member 12	A C-lectin family protein that acts as a scavenger receptor binding to carbohydrate antigens
13	AGT	183	2.90	Angiotensinogen (serpin peptidase inhibitor, clade A, member 8)	Angiotensinogen cleaved by renin to produce angiotensin I
14	SLC16A9	220963	2.82	Solute carrier family 16, member 9 (monocarboxylic acid transporter 9)	A monocarboxylic acid transporter
15	METRN	79006	2.79	Meteorin, glial cell differentiation regulator	A glial cell differentiation regulator
16	CTSH	1512	2.75	Cathepsin H	A lysosomal cysteine proteinase
17	GADD45B	4616	2.70	Growth arrest and DNA-damage-inducible, beta	An environmental stress-inducible protein that activates p38/JNK signaling
18	SAMD11	148398	2.69	Sterile alpha motif domain containing 11	A protein with a SAM motif of unknown function
19	APC2	10297	2.67	Adenomatosis polyposis coli 2	A negative regulator of Wnt signaling
20	SLC2A5	6518	2.63	Solute carrier family 2 (facilitated glucose/fructose transporter), member 5	Glucose/fructose transporter GLUT5
21	GFAP	2670	2.62	Glial fibrillary acidic protein	An intermediate filament protein of astrocytes
22	CCDC103	388389	2.59	Coiled-coil domain containing 103	A coiled-coil domain bearing protein of unknown function
23	C9orf58	83543	2.55	Chromosome 9 open reading frame 58 (ionized calcium binding adapter molecule 2; IBA2)	A calcium binding protein of unknown function
24	CHI3L2	1117	2.52	Chitinase 3-like 2	A secreted chitinase-like protein of unknown function
25	CFI	3426	2.46	Complement factor I	A proteolytic enzyme that inactivates cell-bound, activated C3